

LASER INTERFEROMETER GRAVITATIONAL WAVE OBSERVATORY  
- LIGO -  
CALIFORNIA INSTITUTE OF TECHNOLOGY  
MASSACHUSETTS INSTITUTE OF TECHNOLOGY

Technical Note	LIGO-T1500218-v1	2015/09/08
<b>Prototyping a tilt-free seismometer, Progress Report 2</b>		
Megan Kelley		

**California Institute of Technology**  
**LIGO Project, MS 18-34**  
**Pasadena, CA 91125**  
Phone (626) 395-2129  
Fax (626) 304-9834  
E-mail: info@ligo.caltech.edu

**Massachusetts Institute of Technology**  
**LIGO Project, Room NW22-295**  
**Cambridge, MA 02139**  
Phone (617) 253-4824  
Fax (617) 253-7014  
E-mail: info@ligo.mit.edu

**LIGO Hanford Observatory**  
**Route 10, Mile Marker 2**  
**Richland, WA 99352**  
Phone (509) 372-8106  
Fax (509) 372-8137  
E-mail: info@ligo.caltech.edu

**LIGO Livingston Observatory**  
**19100 LIGO Lane**  
**Livingston, LA 70754**  
Phone (225) 686-3100  
Fax (225) 686-7189  
E-mail: info@ligo.caltech.edu

# 1 Motivation

The Laser Interferometer Gravitational-Wave Observatory (LIGO) experiment uses an enhanced Michelson interferometer to determine the relative distance between two test masses that may be perturbed by a passing gravitational wave. At a frequency of 100 Hz, the displacement sensitivity of LIGO’s 4 kilometer long arms is  $10^{-20}\text{m}/\sqrt{\text{Hz}}$ , which is about five orders of magnitude smaller than the classical radius of the proton.[1] The level of precision required to make this measurement effectively requires that all sources of noise be carefully considered and reduced as far as possible. The three primary sources of noise in the experiment are quantum noise (shot noise) dominant at high frequencies, thermal noise dominant at mid-range frequencies, and seismic noise dominant at low frequencies. The seismic noise begins to dominate at about 10 Hz; lower than 10 Hz the noise increases many orders of magnitude, creating what is known as the “seismic wall” on the low end of LIGO’s sensitivity band, as seen in Figure 1.

The sources of this low frequency noise vary from microseisms (ex. ocean waves minutely pushing on the continent), people walking near the detector, and wind on the detector. There

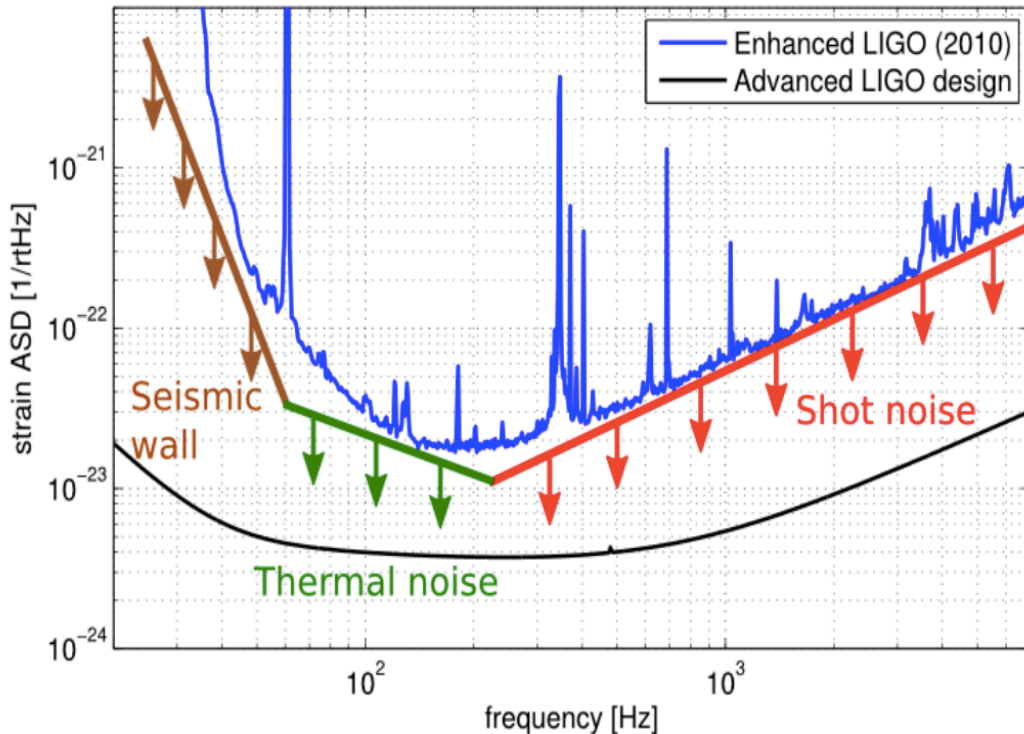


Figure 1: The noise curves for Initial and Advanced LIGO, showing the three main contributors to noise in the three regions.[2]

is great interest in lowering the seismic noise present in the experiment because continuous sources of gravitational waves, such as closely orbiting neutron stars and black holes, emit waves at low ( $<10$  Hz) frequencies. If LIGO can reduce its seismic noise, a greater range of phenomena will be available for study.

The basic structure of a seismometer is that of a mass that can oscillate about an equilibrium, returned by some restoring force. A simple example of this is a mass on a spring. When the ground moves, the mass is forced into oscillation, and some aspects of the ground's motion can be determined from observing the mass's motion. Two aspects of ground motion that are detected with inertial (mass on a spring) seismometers are ground translation and ground tilt. Especially at low frequencies, the tilt component of ground motion contaminates the reading of the seismometer. In present-generation seismometers, the tilt is subtracted out of the signal via a tilt-sensitive instrument. However, the noise in this additional instrument often reduces the precision of the data greatly. Therefore, the end goal of this project is to create a 'tilt-free' seismometer that is mechanically insensitive to tilt, in order to remove the necessity for the second, tilt-only measurement.

As described by Matchard et al.,[3] no inertial sensor can fully distinguish between horizontal translation of the ground and tilt of the ground. However, by clever mechanical design, a sensor that is insensitive to tilt within a certain frequency range can be constructed. The basic design of this sensor is a traditional seismometer in a box that is suspended from a thin wire. The top of the wire is connected to a frame that is rigidly attached to the ground. Assuming a perfect suspension point, the suspended box and seismometer will not move if the ground tilts, and will move if the ground translates. In practice, this method is only effective for ground motion frequencies that are above the resonant frequency of the pendulum formed by the suspended box. So by creating pendula that have very low resonant frequencies, a large range of translational ground motion frequencies can be measured without contaminating tilt motion.

## 2 Summer Project

The project for this summer is to construct a prototype of the theoretical tilt-free seismometer described above. Designs were developed in previous years by Dooley et al.[4]. The design consists of an inverted pendulum on a frame, called the rhomboid, that is suspended from above by thin wires. The relative distance of the inverted pendulum and the rhomboid will be continuously measured via a Michelson interferometer. When the ground translates, the rhomboid is able to swing on its wires, causing the inverted pendulum to move, and register a change of distance in the interferometer. However, when the ground tilts, the orientation of the rhomboid will not change due to its suspension by wires, and no change in distance will be measured by the interferometer. However, due to the fact that no inertial sensor can completely separate tilt and translation, this method is only effective at frequencies above the resonant frequency of the suspended rhomboid.

The interferometer will be a typical Michelson interferometer, in which light travels down two orthogonal arms and is reflected back to the junction of the arms. The resulting interference

of the light when it recombines allows the calculation of the relative distance between two objects (in this case the rhomboid and the inverted pendulum). The lengths of the arms of the interferometer must be accurate to less than 1mm, to reduce frequency noise. Fiber coupled light from another optics table goes to the interferometer, where there will be a 10kHz piezoelectric transducer (PZT) actuator. This PZT is used to modulate the length of one of the arms of the interferometer, which produces a known signal to look for at the asymmetric port. This error signal will be fed back to the PZT after being digitized through a control filter and a digital-to-analog converter.

This prototype seismometer will also include an insulative enclosure and a temperature-control system. The operating temperature of the seismometer will be kept at 35°C, roughly 10°C above room temperature. With the seismometer held above room temperature, it will be isolated from environmental effects such as drafts in the room, heat from other instruments in the room, etc. Higher temperatures are typically a significant source of thermal noise, but in this prototype, priority is placed on keeping the temperature constant. In later incarnations of the seismometer, more advanced temperature control systems will be implemented in order to reduce thermal noise in addition to holding the temperature constant.

The enclosure will consist of aluminum alloy sheets that cover the frame of the seismometer, two flexible silicone-rubber heaters on opposite inside faces, and foam insulation covering the whole of the frame. A ThorLabs temperature controller will be used to keep the temperature at a desired value.

## 3 Project Progress

### 3.1 Thermal Calculations

The frame for the seismometer was constructed from 45mm-square aluminum McMaster-Carr extrusion pieces. It is a simple rectangular prism, 36" high and 27.5" wide and deep. There is a crossbar across the top of the frame, for use in suspending the rhomboid. Once the frame was constructed, the attachment of the aluminum sheets and foam insulation were discussed at great length. The sheets, along with the foam on top of them, will be attached to the frame via drop-in spring-held fasteners to the frame, and ~1" screws. The top portion of the frame, including the cross bar and any supports above it, will be enclosed in a lid made of the same aluminum and foam that surrounds the base. Thus far, all but one face of the enclosure have been constructed. The last face was left off to allow access to the inside of the seismometer, so that the rhomboid and its associated optics can be installed easily.

A thermal time constant for the enclosure was calculated via basic differential equations. Starting from the simple equation  $dQ = mc \cdot dT$  and defining the  $dQ$  as the net flow of energy through the system, the following differential equation was calculated:

$$T'(t) = A - BT(t) \tag{1}$$

where the constants  $A$  and  $B$  are defined as follows:

$$A = \frac{1}{mc}(P_{in} - KA_{side}d_{insul}T_{lab}), \quad B = \frac{KA_{side}d_{insul}}{mc} \tag{2}$$

where  $P_{in}$  is the power delivered into the system by the heaters,  $K$  is the K-factor of the insulation,  $d_{insul}$  is the thickness of the insulation,  $T_{lab}$  is the constant temperature of the lab room,  $A_{side}$  is the area of one face of the frame,  $m$  is the mass of the frame and outer layers, and  $c$  is the specific heat of aluminum. Solving equation (1) yields the following:

$$T(t) = \frac{A}{B} + C_1 e^{-Bt} \quad (3)$$

which implies that the time constant for the system is the inverse of  $B$ . Using estimates for the parameters of the system (seen in Table 1), the time constant was calculated to be 2.25 hours. This is longer than the desired 500 second time constant, so the parameter space of the system must be explored in order to yield a lower time constant.

$K$	Thermal conductivity of insulation	58.121 $J/K/s/m^2/m$
$A_{side}$	Area of one enclosure side	0.75 $m^2$
$d_{insul}$	Thickness of insulation	0.0254 $m$
$m$	Mass of one side of enclosure's frame	10 $kg$
$c$	Specific heat of aluminum	0.9 $J/g/K$

Table 1: Values used in determining the time constant of the thermal enclosure.

### 3.2 Small-Scale Thermal Enclosure Testing

The initial tests of the materials used in the construction of the thermal enclosure were done on a small scale. A small ( $\sim 6''$  square by  $1''$  high) hollow box made of aluminum was surrounded by the lightweight melamine insulation that is used in the full-scale enclosure. A small  $1''$  by  $5''$  Kapton resistive heater was adhered to the inside upper face of the aluminum box, and a thermistor was adhered near it. The heater and the thermistor were connected to a ThorLabs TC200 temperature controller.

With only the sides of the aluminum box insulated, the system took about 20 minutes to equilibrate from room temperature to  $35^\circ\text{C}$ . With all faces of the box insulated, the equilibration time was about 15 minutes. This small-scale test demonstrated the time constant's dependence on both the insulation of the system and the power output by the heater. With less insulation, heat could more easily leak out of the system, increasing the time constant. Thus, the time constant is inversely proportional to the amount of insulation on the enclosure. And with more power output by the heaters, the system reaches the set temperature more quickly, so the time constant is also inversely proportional to the power output by the heaters.

### 3.3 Full-Scale Heater Testing

The heaters used in the full-size enclosure are  $6''$  by  $24''$  flexible silicone-rubber heat sheets from McMaster Carr. To carry out an initial test, the heaters were wired in series and placed under a section of aluminum siding and between sheets of foam. The heaters were then driven with the TC200 temperature controller from room temperature ( $23.7^\circ\text{C}$ ) to a

final set temperature (35°C). At the time of writing, there is no way to get temperature-vs.-time data from the TC200 controller, so for the initial heater test data was taken by hand. The data from this test is shown in Figure 2.

The blue line in Figure 2 represents the actual temperature of the enclosure, and the green line represents a theoretical  $1 - e^{-t}$  heating curve, with a time constant of 25 minutes. Because the time constant value represents the time it takes for an increasing-temperature system to reach  $1 - 1/e \approx 63.2\%$  of its final asymptotic value, the time constant of the temperature data can be calculated directly. The time constant value calculated, 25 minutes, was then used to fit the theoretical curve to the data.

After matching relatively closely between 20 minutes and 50 minutes, the theory and the data begin to diverge around the 55 minute mark. This is due to the fact that the data curve eventually reaches the set temperature, while the theory curve only ever asymptotically approaches the set temperature. The differences between these two curves show that the TC200 controller does more than apply a constant power to the heaters until they reach the set temperature; further tests will be needed to determine the controller's process for bringing materials to a given set temperature.

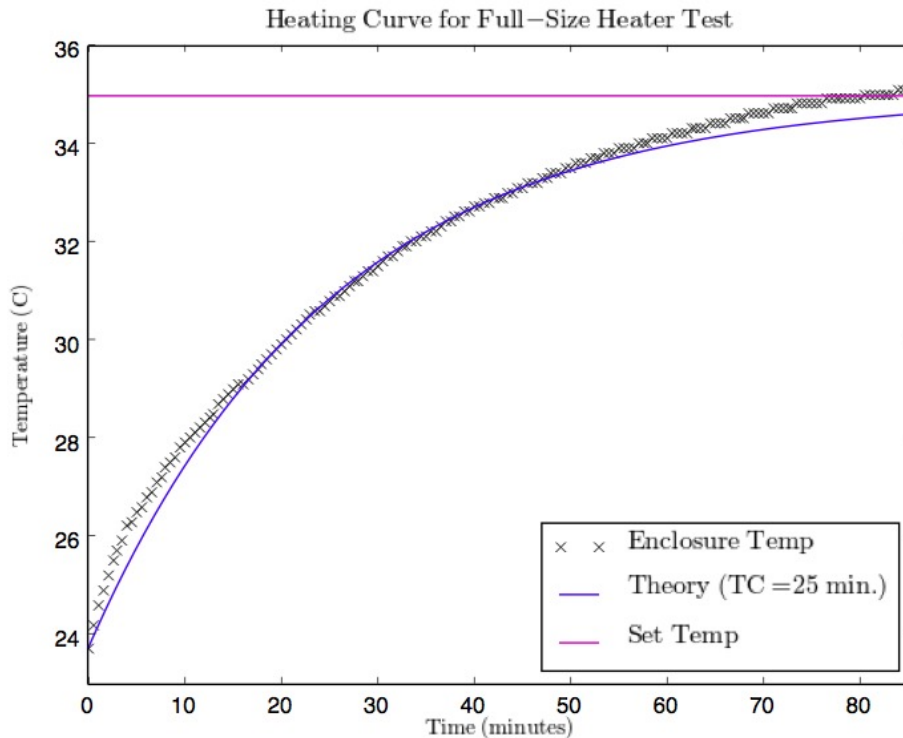


Figure 2: Temperature of the setup as a function of time for the initial test of the full-size heaters.

### 3.4 Rhomboid Suspension

The rhomboid has been suspended from the outer frame using high-carbon steel wires, secured at the lower end with pin vises and at the upper end with pin vises and plate clamps. A first attempt to suspend the rhomboid resulted in a broken pin vise, but after using epoxy to secure it, the rhomboid was successfully suspended and remained suspended for a long period of time ( $\sim$ weeks). A new design for wire clamping has been devised; in this new design a collet surrounds the wire, and is tightened around the wire via a small opening in a block of aluminum. The tension from the weight of the rhomboid is counteracted by a peg attached to a worm gear, similar to tuners used on string instruments. This new wire suspension will be implemented on the next iteration of the rhomboid.

Initially, the rhomboid had a very low resonant frequency of about 40 mHz. The tens of millihertz range approaches frequencies that are very challenging to achieve in mechanical devices, which bodes well for this design. As optical devices were added to the rhomboid, the resonant frequency increased to about 100 mHz. To counteract this, counterweights were added to balance the rhomboid and return it to its initial resonant frequency. The center of mass of the bare rhomboid is designed to be about 1 mm below the wire connection point, which keeps the system stable. When the optics were added, the center of mass rose above the connection point, which made the pendulum's motion unstable. To combat this, counterweights were added to the bottom-most face of the rhomboid. These weights kept the rhomboid hanging evenly, and also ensured that there would be a restoring force returning the rhomboid to equilibrium.

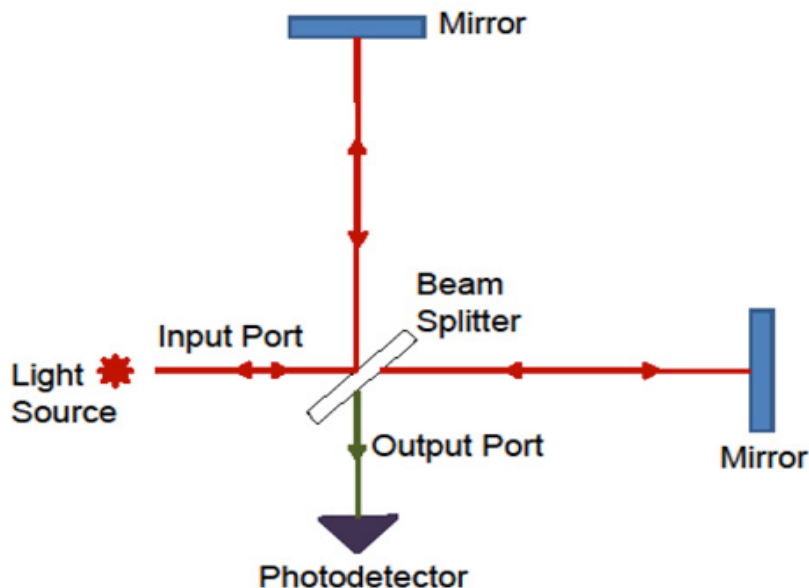


Figure 3: A diagram explaining a typical Michelson interferometer.

### 3.5 Michelson Interferometer

The Michelson interferometer itself will be constructed from two  $0^\circ$  incidence end-mirrors, one  $45^\circ$  incidence beam splitter, and two  $45^\circ$  incidence steering mirrors. A 500 mW, 1064 nm laser will be used to operate the Michelson. The laser is nominally 500 mW, but due to old age its true power is somewhat less. Additionally, the light travels through several waveplate/beamsplitter junctions, which reduces the beam power to  $\sim 75$  mW once it reaches the fiber. Once the light has been directed into the fiber, the fiber travels between the optics table and the seismometer itself.

In comparison with Figure 3, the end mirror attached to the inverted pendulum is represented by the rightmost mirror. The second end mirror, the beamsplitter, and the photodetector are all attached to the rhomboid. The source of the laser light is the output of a fiber, which is also attached to the rhomboid.

## 4 Project Challenges

The biggest challenge of the project has been the design of the thermal enclosure. The basic design, including the layered structure of frame, aluminum sheeting, heaters, and insulation, was well-defined, so the challenges have lain in the specifics of fitting all the layers together. The initial design was to have one sheet of aluminum per face of the frame, but after cutting the aluminum sheeting too short, the design was modified to include a separate lid component. An added benefit of the lid is accessibility: it offers the ability to access the inside of the seismometer without having to completely remove one of the side panels.

Another challenge has been the behavior of the suspended rhomboid. When first suspended, it did not hang straight down from the suspension point, rather, it twisted slightly around its two support wires. It also hung slightly higher to one side than the other. The twisting could be due to a wire being attached when it was not fully unwound, and the uneven hang could be due to uneven upper pin vises. Re-suspending the rhomboid after confirming that the wires are not twisted on themselves may fix the twisting problem, while careful weight distribution will fix the uneven hang.

Finally, the placement of the Michelson interferometer on the rhomboid and inverted pendulum poses a challenge because of weight distribution issues. All of the Michelson's components will be placed on the upper face of the rhomboid, which will bring the center of mass of the rhomboid/inverted pendulum system above the suspension point. This can be counteracted with counterweights on the bottom of the rhomboid, but the major challenge lies in balancing the system in such a way that the resonant frequency of the system is low ( $\sim 40$  mHz). The Michelson is still in construction, so this challenge will be confronted, and possibly resolved, in the remainder of the summer.



## References

- [1] Abramovici, A.; Althouse, W. E.; Drever, R. W. P.; Gürsel, Y.; Kawamura, S.; Raab, F. J.; Shoemaker, D.; Sievers, L.; Spero, R. E.; Thorne, K. S.; Vogt, R. E.; Weiss, R.; Whitcomb, S. E.; Zucker, M. E., *LIGO: The Laser Interferometer Gravitational-Wave Observatory*. Science, 256, 325-333, 1992.
- [2] Dooley, K. *Seismic Isolation*. Presentation for LIGO SURF, DCC G1500851-v1, 2015.
- [3] Matichard, F.; Mittleman, R.; Evans, M., *On the mechanical filtering of the transmission of tilt motion from ground to horizontal inertial sensors*. Pre-print for submission to the Bulletin of the Seismological Society of America (2015).
- [4] Dooley, K.; Moon, S.; Arai, K.; Adhikari, R., *Towards a tilt-free seismometer design*. Poster at March LVC Meeting (2015), DCC G1500315-v1.